URTeC: 2671301

Mapping Unconventional Reservoir Stress Conditions: An Integrated Workflow Using Geological, Stimulation and Microseismic Data

Orlando J. Teran, MicroSeismic Inc.

Summary

In this study we present a geomechanical analysis workflow using microseismic focal mechanisms to investigate the dynamic response of the reservoir during and after stimulation. Focal mechanisms are derived using full waveform fitting techniques, and the ambiguity in identifying the true fracture plane is resolved by simply choosing the nodal plane that aligns with the developing hydraulic fractures. A global stress inversion of the fracture plane solutions is done to estimate the orientations and relative magnitudes of the principle stresses. Friction laws are then used to constrain for each event a suite of geomechanical parameters (failure potential, dilation tendency, and excess pore pressure) in order to identify fracture populations likely to control fluid flow, those that required different stimulation pressures in order to contribute to flow, and the mechanical conditions that favored out-of-zone growth and reactivation of geohazards. Additional observations, such as net wellbore pressure measurements and geophysical logs, are used to calibrate the model as well as to further understand the geological, geomechanical and treatment-related variables affecting the overall stimulated rock volume. The method is applied and discussed in the case of a microseismic event catalogue obtained during the stimulation of two horizontal wells landed in the Eagle Ford, where large variations in fracture patterns as well as the reactivation of a large macroscopic fault zone was observed.

Introduction

The state of stress of the reservoir is one of the dominant factors controlling the reservoirs response to stimulation as well as the effectiveness of the treatment design. For instance, the orientation and magnitude of the maximum horizontal stress (SHmax) strongly affects the stimulated range of fracture orientations and in turn the geometry of the stimulated zone (i.e. localized versus distributed fracturing). The hydraulic horsepower, which takes into account the reservoir stress states and pressures, may be sufficient to stimulate parts of the reservoir with a specific state of stress, but any variations in the stress state can result in adverse effects such as damaging nearby wells (“frac hits”), out-of-zone growth, and large-magnitude earthquakes. Furthermore, the reservoir stress state can also impact the hydraulic conductivity of stimulated fractures (Barton et al., 1995).

In this study a catalogue of microseismic focal mechanisms is used to map the stresses onto the microseismic fracture planes and evaluate the states of stress throughout the stimulated rock volume. The microseismic catalogue was obtained from a surface array of geophones designed to monitor a two-well zipper frac landed in the lower Eagle Ford. The advantage of the surface array of geophones is that it provides ample coverage and sampling of the focal sphere that results in very robust focal mechanism [FM] solutions (this is versus downhole monitoring arrays, which only sample a fraction of the focal sphere). Using full-waveform fitting techniques the FM for each microseismic event with sufficient signal-to-noise ratio was auto-picked resulting in a catalogue of ~1,800 unique solutions. For each solution the true fracture plane was identified and this was then used to invert for the orientation and relative magnitude of the maximum horizontal stress. Then, using the derived stress tensor and the Mohr-Coulomb failure criterion, the shear and normal stresses were calculated for each of the fracture plane solutions and its fracturing potential (with an assumed friction coefficient). This results in a dense spatial sampling of the stress states throughout the stimulated volume. Next, the stimulation potential (i.e. the amount of pressure required to

stimulate the observed fractures) was derived along the laterals and compared to the instantaneous bottomhole shut-in pressures. As will be shown below, the purpose of this workflow is to demonstrate how microseismic fracture planes permit a rapid assessment of the states of stress throughout the stimulated reservoir in order to understand the geologic and engineering factors responsible for the observed fracturing and, ultimately, the predictability of the frac.

Results

The catalogue of fracture plane solutions [FPS] revealed variations in the stimulated fracture systems that range from linear and simple geometries to geometrically complex patterns (i.e. multiple fracture orientations) as well as the reactivation of a presumably large fault zone (Figure 1A). The dominant fracture system observed from the FPS catalogue is characterized by simple-type fracture patterns that are defined by subparallel fractures with dip-slip kinematics that tend to localize along linear zones (Figures 1A and 1C). Two subpopulations in FPS with distinctly different orientations and kinematics were observed near the toe and towards the heel of the wells. At the toe of the wells the microseismic events revealed the reactivation of a large fault and here the FPS have orientations that subparallel the structural feature and strike-slip kinematics (Figures 1A and 1B). This observation shows that 1) the reactivation of this geohazard could have been mitigated in real-time, and 2) the coexistence of these two types of movements is a good indicator of a relatively high horizontal stress anisotropy. Another interesting aspect of the fracture systems in this reservoir is that towards the heel of the wells the FPS data changes from the simple-type fracture geometries to a geometrically complex fracture system with a much larger range of fracture orientations and styles of movement (Figures 1A and 1D). This change in fracture geometries is most likely controlled by the geology and, as will be shown below, represents a different state of stress.

The state of stress of a fracture depends on its orientation and friction in a given stress field, and the microseismic FPS catalogue shows a gamut of stress states throughout the reservoir (Figures 2A and 2B). The simple fracture patterns are generally critically stressed, suggesting that these fractures were easier to stimulate and, according to Barton et al., (1995), these should also be the most hydraulically conductive. The zone of geometrically complex fracture patterns are dominated by non-critically stressed fracture orientations, and could possibly be less conductive to flow. The fault-related FPS indicate that this feature has an orientation that is subcritically stressed under this stress field, and the FPS near the intersection between the fault and the wellbore span the full range of stress states suggesting that the fault may have been easier to stimulate than this part of the reservoir (assuming the differences in friction coefficients between the two zones is not large).

The stimulation potential derived using the FPS, the stress tensor and friction coefficient shows that the relative pressures required for the observed fracturing correlates well with spatial variations in the FPS (Figures 2C, 2D and upper and middle panels in Figure 3). The stimulation pressure is defined here as the amount of pressure required to fail a fracture of any orientation and is measured relative to the most critically stressed fracture orientation (here we assume negligible cohesion and a friction coefficient of 0.6) and normalized to the mean stress. This analysis indicates that the fault related FPS required a ~15% increase in pressure, whereas the FPS at the location where the fault was breached required much higher stimulation pressures (up to 35%) suggesting that the treatment design here favored the reactivation of the fault. Along sections of the wellbores where the simple-type fracture patterns were observed the required stimulation pressures were generally <10%, whereas, the zone of geometrically complex fracture patterns, the stimulation pressures were much higher (~35-40%). These observations together demonstrate the variations in the hydraulic horsepower required to stimulate different parts of the reservoir as well as to avoid geohazards. A comparison of the instantaneous shut-in pressures measured along the laterals also shows a positive correlation with the variations in stimulation pressures measured from the FPS (bottom panel in Figure 3), which can be interpreted as possible variations in mechanical rock properties. Although the absolute values of the stress magnitudes were not used, these observations demonstrate a positive correlation between the actual pressure injected into the fracture at the point of failure and the mechanical conditions required to fail a fracture of any orientation.

Conclusions

In this paper a geomechanical analysis was performed on a large catalogue of microseismic focal mechanisms recorded from a surface array of geophones. It was demonstrated that the fracture plane solutions obtained from microseismic monitoring permit a rapid assessment of the stress conditions throughout the stimulated volume and reveal important implications about the treatment design and the geologic variations. The positive correlation

observed between the actual fracture pressures (i.e. ISIP) and the stimulation potential of the observed fracturing suggests a possible predictability of which fractures will fail under different treatment designs. It is important to note that this study assumed a constant stress field, however, it is well known that the in situ stress field can vary locally during stimulation, and further work will be to investigate the spatio-temporal stress perturbations using the microseismic focal mechanisms. Additional work will also include integrating the absolute values of the principal stresses along with a measured coefficient of friction to further test the reliability of the equations governing rock failure in applications such as real-time monitoring and mitigation of geohazards, stress-strain-dependent fracture permeability, among the many other stress-dependent variables that can affect the integrity of the stimulated volume.

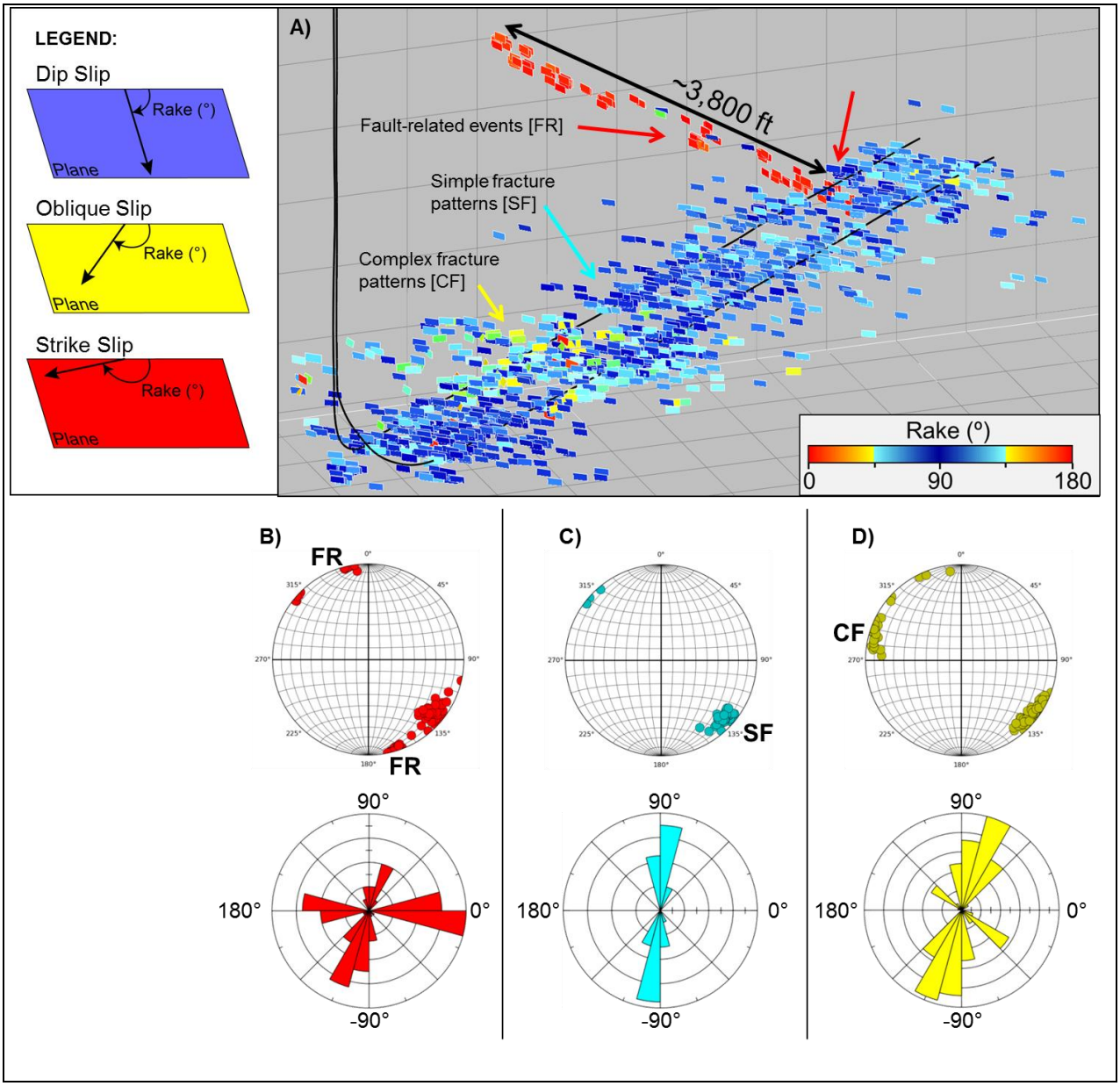

Figure 1: A) Oblique view of the catalogue of microseismic fracture plane solutions obtained from the treatment of two hoizontal wells (shown in black) in the lower Eagle Ford. Fracture planes are colored by their rake vectors, which is explaied in the legend to the left of figure. B), C) and D) Upper plots are lower hemisphere stereonets showing poles to the fracture planes and lower plots are rose diagrams showing the distribution of the rake vectors measured at the red, cyan and yellow arrows, respectively, shown in A).

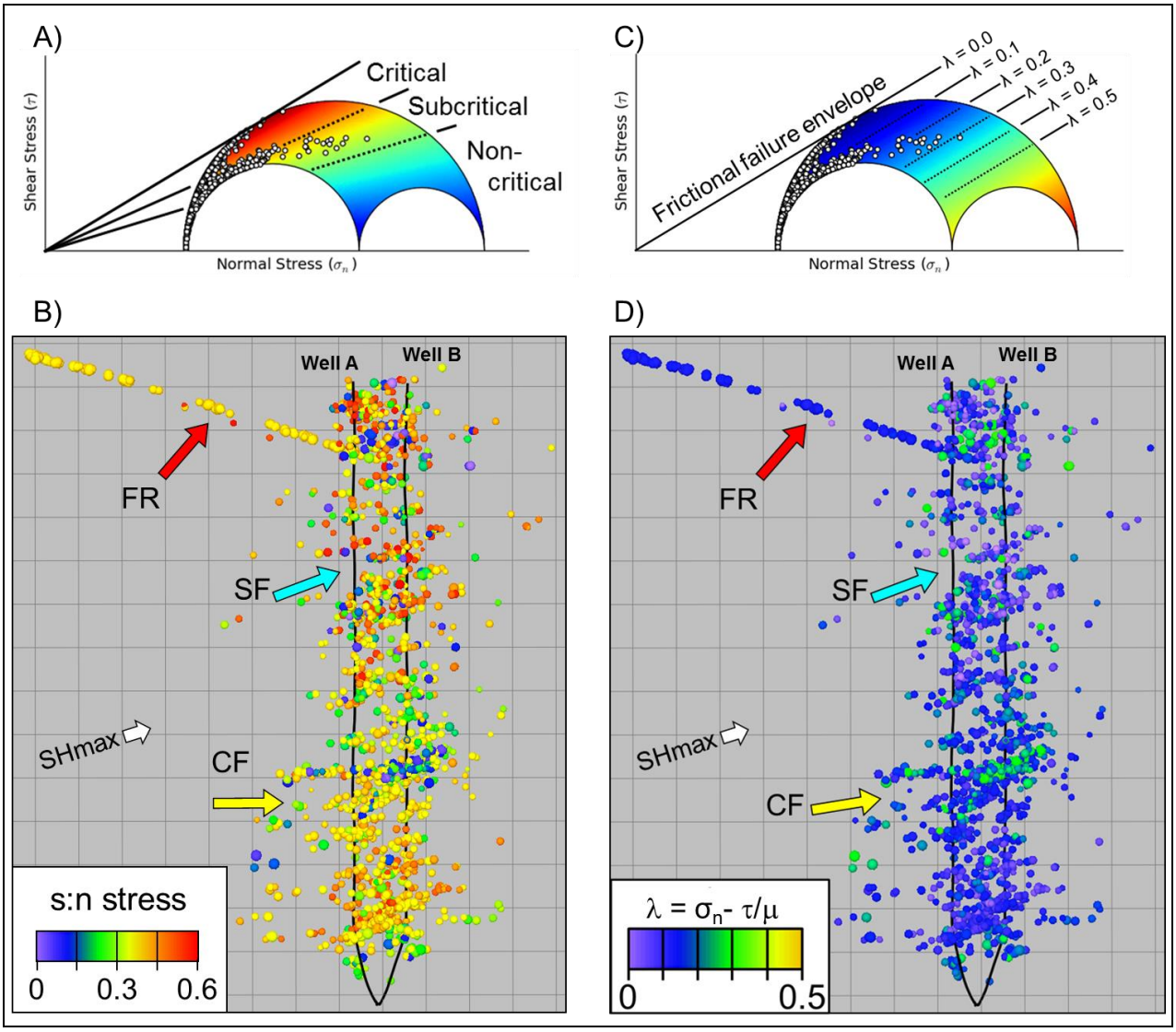

Figure 2: A) Mohr diagram highlighting the states of stress of the hydraulic fracturing microseismicity. B) Mapview of the microseismic events styled by their shear:normal stress ratio. A) and B) share the same color scheme. C) Mohr diagram showing the stimulation potential as a function of increasing fluid pressure normalized the mean stress. D) Mapview of the microseismic events styled by the stimulation potential. C) and D) share the same color scheme. FR – fault related; SF – simple-type fracture patterns; CF – geometrically complex fracture patterns; SHmax – orientation of maximum horizontal stress.

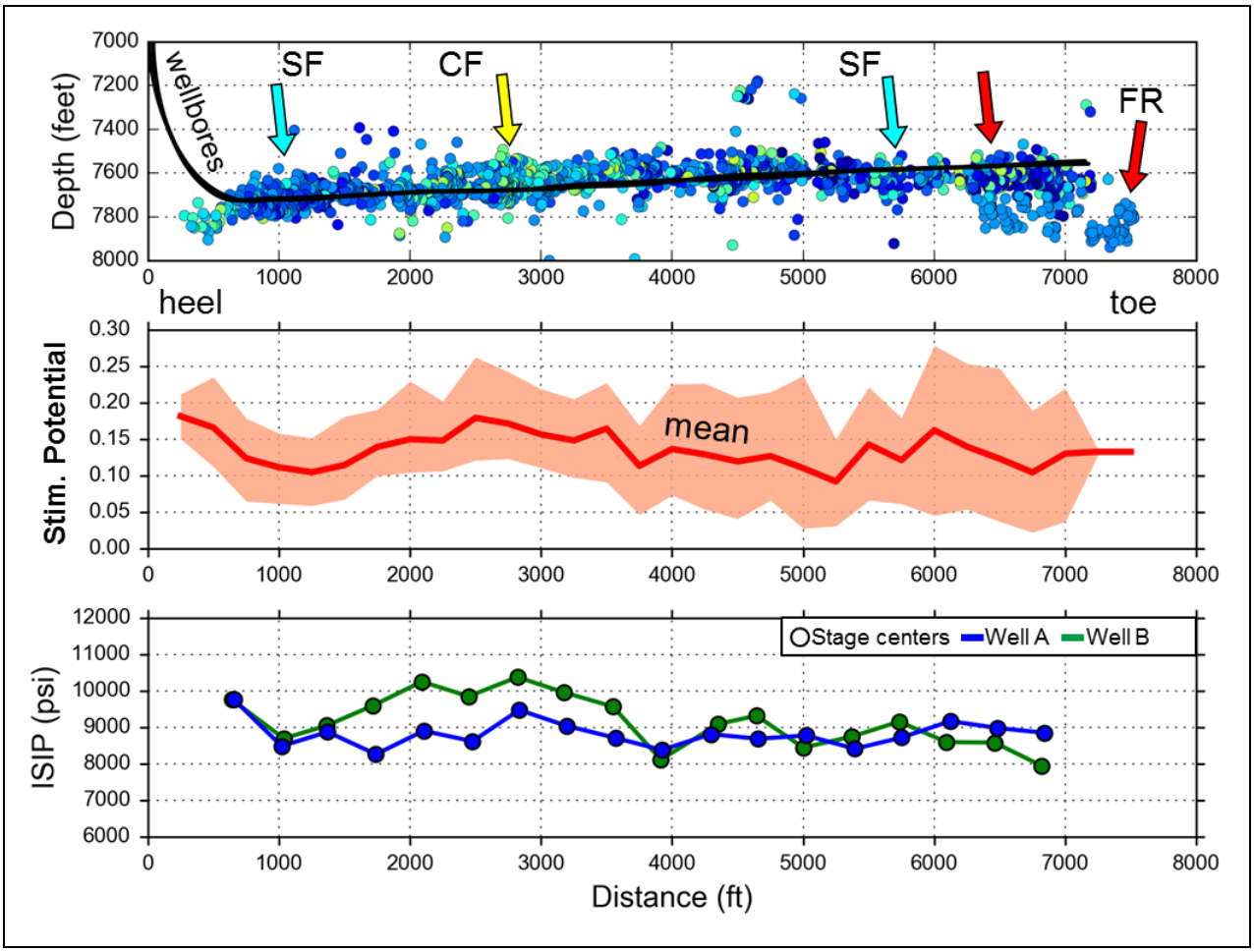

Figure 3: Upper plot is a depth profile of the wellbores and the microseismic events colored by the stimulation potential. Middle plot shows the statistical range of stimulation potentials sampled along the length of the wellbores. Lower plot shows the instantaneous shut-in pressures measured along both wells, and when compared to the middle plot, the ISIP shows similar variations.

References

Barton, C.A., Zoback, M.D., Moos, D., 1995, Fluid flow along potentially active faults in crystalline rock. Geology. v23p.683-686